Acrylamides with hydrolytically labile carbonate ester side chains as versatile building blocks for well-defined block copolymer micelles via RAFT polymerization

*Sabah Kasmi[a], Benoit Louage[a], Lutz Nuhn[a], Glenn Verstraete[a], Simon Van Herck[a], Mies J. van Steenbergen[b], Chris Vervaet[a], Wim E. Hennink[b], Bruno G. De Geest[a]**

[a] Department of Pharmaceutics, Ghent University, Ghent, Belgium

[b] Department of Pharmaceutics, Utrecht Institute for Pharmaceutical Sciences, Utrecht University, Utrecht, The Netherlands

* corresponding author: Prof.Dr. Bruno G. De Geest

Department of Pharmaceutics, Ghent University

Ottergemsesteenweg 460, 9000 Ghent, Belgium

e-mail: br.degeest@ugent.be

phone: +32 9 264 80 55

Abstract

En route towards improved delivery systems for targeted chemotherapy, we propose a straightforward approach for the hydrophobic modification of the acrylamide *N*-(2-hydroxyethy)acrylamide (HEAm). An ethyl or benzyl group was introduced via a hydrolytically sensitive carbonate ester yielding HEAm-EC and HEAm-BC, respectively. Block copolymers of HEAm, respectively PEG and HEAm-EC or HEAm-BC were successfully synthesized by reversible addition-fragmentation chain transfer (RAFT) polymerization, obtaining a library of well-defined block copolymers with different degrees of polymerization (DP). To further explore the versatility of our approach in terms of polymer synthesis, self-assembly, drug solubilization and *in vitro* cell interaction, polyethylene glycol (PEG) and polyHEAm as hydrophilic polymer blocks were compared. The block copolymers formed micellar nanoparticles (10-100 nm) in PBS and could efficiently solubilize hydrophobic dyes and anti-cancer drugs. Benzyl carbonate ester side chains increased micellar stability and drug loading capacity. Moreover, PEG as hydrophilic block showed in comparison to HEAm more promising results concerning both colloidal stability and drug loading capacity. Confocal microscopy showed that the micelles could efficiently deliver a hydrophobic dye inside the cells. Finally, we also demonstrated efficient formulation of the anti-cancer drug paclitaxel with an *in vitro* cancer cell killing performance comparable or even better than the two commercial PTX nanoformulations Abraxane and Genexol-PM at equal drug dose. In conclusion, modification of HEAm through carbonate linkages offers a versatile platform for the design of degradable polymers with potential for biomedical applications.

1. Introduction

In the past decades, polymeric micelles have been extensively studied as drug delivery carriers for poorly water-soluble drugs. Moreover they are of great interest because of their high loading capacity, size (10-100 nm), biocompatibility and chemical versatility.[1,2,3,4,5] Polymeric micelles, which consist of a hydrophilic outer shell and hydrophobic inner core, are attractive systems for the delivery of a drug payload to tumors via a combination of targeting, mediated by active – ligand-receptor interactions and by passive enhanced permeability and retention (EPR) effect[6]. The former aims at enhancing the delivery to cancer cells that overexpress a specific receptor. The latter, first reported in 1986 by Maeda et al[7], allows extravasation and retention of the micelles in tumor tissue, which in turn leads to higher drug concentration and increased therapeutic efficacy.[8–10]

En route towards improved delivery systems for targeted chemotherapy we previously reported on the modification of *N*-(2-hydroxypropyl)methacrylamide (HPMA) with an ethyl group via a hydrolytically sensitive carbonate ester (i.e. HPMA-EC) which was polymerized by free radical polymerization (FRP) using a PEG-based macroinitiatior.[11] Introduction of a hydrophobic moiety onto the hydroxyl group of HMPA renders the corresponding polymers more hydrophobic which could be used as driving force for temperature-induced self-assembly into micelles of PEG-poly(HPMA-EC) block copolymers in aqueous medium. Moreover, hydrolysis of the carbonate esters afforded fully soluble polymers, suggesting transiently thermoresponsive[5] properties of the polymers

Here, we vastly expand upon our previous work on different levels. On the level of the route of polymerization we elaborate in the present work on controlled radical polymerization rather than FRP due to the limited control on polymer molecular weight and molecular weight distribution offered by FRP. Reversible addition-fragmentation chain transfer (RAFT) polymerization is more favorable to obtain polymers with controlled molecular weight, low dispersity and end-group functionality[9,12].

On the monomer level we devised an alternative strategy for the synthesis of carbonate-modified hydroxyl-containing monomers which allowed us to extent our approach to acrylamides, which were previously inaccessible due to the occurrence of Michael addition as a side reaction. The use of acrylamides yields access to well defined block copolymers which – at least in our hands – could not be obtained by methacrylamides, which showed, in particular when attempting block copolymer synthesis, slow polymerization kinetics and limited end group fidelity. Similarly mixed success with RAFT block copolymerization of methacrylamides has also been reported by other groups.[13–15] Therefore we opted in this work to elaborate on the use of *N*-(2-hydroxyethyl)acrylamide (HEAm) as monomeric scaffold for modification at its hydroxyl position with carbonate esters.

Third, we propose in the present work the modification of HEAm with ethyl – yielding HEAm-EC – and benzyl – yielding HEAm-BC – side chain via a carbonate ester. The use of an ethyl side chain extends onto previously reported strategy for HPMA modification to the level of acrylamides, whereas benzyl modification is a new avenue we explore in this work to render the micelles more stable by promoting hydrophobic interactions in their core. The latter should increase micellar stability and drug loading capacity, due to π-π stacking of the aromatic groups, which was also demonstrated by Shi et al. [16,17] Starting from respectively ethanol and benzyl alcohol that are tethered to HEAm via a carbonate ester moiety, we aim at the design of polymeric building blocks that are degradable into the same benign products that should not pose issues of long term accumulation in the body.

In a first attempt to evaluate the potential of these materials in a biomedical context, we synthesized block copolymers composed of HEAm-EC, respectively HEAm-BC, as hydrophobic block and several types of hydrophilic polymer blocks to explore the versatility of our approach in terms of polymer synthesis, self-assembly, drug solubilization and *in vitro* cell interaction.

2. Experimental section

2.1. Materials

All chemicals were purchased from Sigma Aldrich unless mentioned otherwise. The RAFT-CTA 2-(butylthiocarbonothioylthio)propanoic acid (PABTC) was synthesized according to literature.[18] TLC plates were purchased from Macherey Nagel. Dulbecco's Phosphate-buffered saline (DPBS) (pH 7.4, 0.14 M NaCl, 1.5 mM KH_2PO_4, 8.1 mM Na_2HPO_4 * 7 H_2O) was purchased from Thermo Fisher Scientific.

Paclitaxel (PTX) was obtained from LC Laboratories. Octadecyl Rhodamine B Chloride (R18), enzyme-free Cell Dissociation Buffer, Dulbecco's Modified Eagle Medium (DMEM), fetal bovine serum (FBS), L-glutamine, sodium pyruvate, penicillin, streptomycin, Hoechst, Alexa Fluor 488 and Phalloidin were obtained from Invitrogen. SKOV-3 cells were supplied by ATCC.

2.2. Instrumentation

^{1}H-Nuclear Magnetic Resonance (NMR) spectra were recorded on a Bruker 300 MHz FT-NMR spectrometer using $CDCl_3$ and d^6-DMSO as solvents. Chemical shifts (δ) are given in ppm relative to TMS.

Electron spray ionization-mass spectroscopy (ESI-MS) was carried out on a Waters LCT Premier XETM TOF mass spectrometer with a ZsprayTM source and ESI and modular LocksprayTM interface, coupled to a Waters alliance HPLC system.

Size exclusion chromatography (SEC) was performed on a Shimadzu 20A system, equipped with a 20A ISO-pump and a 20A refractive index detector (RID). Measurements were executed in *N*,*N*-dimethylacetamide (DMA), containing 50 mM LiBr at 50 °C with a flow rate of 0.700 mL/min. Samples were run with toluene as an internal standard. Calibration of the 2 PL 5 µm Mixed-D columns was done with polymethylmethacryate (PMMA- standards) obtained from PSS (Mainz).

Dynamic light scattering (DLS) was performed on a Zetasizer Nano S (Malvern Instruments Ltd., Malvern, U.K.) equipped with a HeNe laser (λ = 633 nm) and detection at scattering angle of 173°. Cumulants analysis of the data gave the z-average and polydispersity index and data fitting by CONTIN the particle size distribution. PBS was used as buffer.

Fluorescence spectroscopy was carried out on a Cary Eclipse fluorescence spectrophotometer (Agilent Technologies) equipped with a Varian Cary Temperature Controller.

Turbidimetry measurements were performed in a CARY Bio 100 UV–VIS spectrophotometer equipped (Agilent Technologies, Santa Clara, CA, USA) with a temperature controller, at a wavelength of 700 nm.

Heating/cooling cycles were performed at a rate of 1 °C/ min with stirring. The polymer concentration was kept at 5 mg/mL in PBS

Confocal microscopy images were recorded on a Leica DMI6000 microscope coupled to an Andor DSD2 scanner and a Zyla5.5 CMOS camera. 2D cell cultures were imaged with a 1.40 NA 63x oil immersion objective. 3D spheroids were imaged with a 10 x objective. Images were processed with ImageJ.

High-performance liquid chromatography (HPLC**)** analyses were done on a system with an isocratic solvent pump (L-7100, Merck, Hitachi LaChrom, Tokyo, Japan) set at a flow rate of 1 mL/min, an autosampler (L-7200, Merck, Hitachi LaChrom, Tokyo, Japan) with a loop of 100µL, a guard column (RP 18e) followed by a reversed phase C18 column (LiChroCart® 250-4, LiChrospher® 100 RP (5 µm)) and a UV-detector (L-7400, Merck, Hitachi LaChrom, Tokyo, Japan) set at a wavelength of 207 nm. The mobile phase consisted of water/acetonitrile (60/40) and the injection volume was set at 10 µL.

Ultra-performance liquid chromatography (UPLC) analyses were carried out using Waters Acquity system consisting of a binary solvent manager, a sample manager and a UV detector. An Acquity UPLC BEH C18 1.7 µm column (2.1 x 50 mm) was used with a column temperature of 50°C. The mobile phase consisted of acetonitrile/water 45/55 (v/v), supplemented with 0.1% (v/v) trifluoroacetic acid at a flow rate of 1 mL/min.

2.3. Synthesis of HEAm-BC

The synthesis of HEAm-BC was performed in 2 steps and was based on the protocol for the synthesis of HEMA-CI and HPMA-EC.[11,19] First, a round-bottom flask was filled with 1,1'-carbonyldiimidazole (CDI) (4.86 g, 30.0 mmol) and 25 mL anhydrous dichloromethane under a nitrogen atmosphere. Subsequently, benzylalcohol (2.07 mL, 20.0 mmol) was added after which a clear solution was obtained. After 2 h stirring at room temperature, the reaction mixture was transferred into a separatory funnel and washed with water. The dichloromethane layer was dried over $MgSO_4$ and filtered. The solvent was removed under reduced pressure, yielding the activated monomer as yellow oil (quantitative). ^{1}H-NMR activated benzylalcohol (BC-CI) ($CDCl_3$, 300 MHz), δ (ppm): 8.07 (s, 1H, imi-H), 7.36 (m, 6H, imi-H, benzyl-H), 6.99 (s, 1H, imi-H), 5.35 (s, 2H, C-CH_2).

In the next step the activated benzylalcohol (4.30 g, 21.26 mmol) was dissolved in 10 mL anhydrous DMF under a nitrogen atmosphere. *N*-(2-hydroxyethy)acrylamide (HEAm, 4.896 g, 42.52 mmol), also dissolved in anhydrous DMF, was added dropwise. Note that HEAm contained 1,000 ppm monomethyl ether hydroquinone as inhibitor, which proved sufficient to prevent autopolymerization. Moreover, we confirmed by ^{1}H-NMR, that after rotary evaporation of the reaction mixture, but before manual column chromatography purification, no autopolymerization occurred. The reaction mixture was stirred overnight at 80 °C. Afterwards the solvent was evaporated under reduced pressure and the product was redissolved in dichloromethane. The dichloromethane layer was washed with 1M HCl in water to remove formed imidazole. The dichloromethane layer was dried over $MgSO_4$ and filtered. Lastly, the residual reaction mixture was purified using silicagel column chromatography (eluent dichloromethane/ethyl acetate – 9/1 (v/v)) (yield: 60%) ^{1}H-NMR HEAm-BC ($CDCl_3$, 300 MHz), δ (ppm): 7.32 (m, 5H, benzyl-H), 6.21 (dd, 1H, CH_2=*CH*), 5.99 (dd, 1H, *CH_2*=CH), 5.86 (br, 1H, *NH*), 5.58 (dd, 1H, *CH_2*=CH), 5.10 (s, 2H, O*CH_2*C), 4.20 (t, 2H, O*CH_2*CH_2), 3.56 (q, 2H, OCH_2*CH_2*). ESI-MS $C_{13}H_{14}NO_4$: calculated $[M + H]^+$ 250.10738, $[M + Na]^+$ 272.08932, $[M + K]^+$ 288.06326, found $[M + H]^+$ 250.1062, $[M + Na]^+$ 272.0881, $[M + K]^+$ 288.0615.

2.4. Synthesis of HEAm-EC

A round-bottom flask was filled with 1,1'-carbonyldiimidazole (CDI) (4.86 g, 30.0 mmol) and 25 mL anhydrous dichloromethane under a nitrogen atmosphere. Subsequently, ethanol (1.17 mL, 20.0 mmol) was added after which a clear solution was obtained. After 2 h stirring at room temperature, the reaction mixture was transferred into a separatory funnel and washed with water. The dichloromethane layer was dried over $MgSO_4$ and filtered. The solvent was removed under reduced pressure, yielding the activated monomer as a clear oil (quantitative). ^{1}H-NMR activated ethanol (Et-CI) ($CDCl_3$, 300 MHz), δ (ppm): 8.07 (s, 1H, imi-H), 7.36 (s, 1H, imi-H), 7.00 (s, 1H, imi-H), 4.42(q, 2H, *CH_2*-CH_3), 1.37 (t, 2H, CH_2-*CH_3*).

In the next step the activated ethanol (2.98 g, 21.26 mmol) was dissolved in 10 mL anhydrous DMF under a nitrogen atmosphere. *N*-(2-hydroxyethy)acrylamide (4.896 g, 42.52 mmol), also dissolved in anhydrous DMF, was added dropwise. The reaction mixture was stirred overnight at 80 °C. Afterwards the solvent was evaporated under reduced pressure and redissolved in dichloromethane. The dichloromethane layer was washed with 1M HCl in water to remove formed imidazole. The dichloromethane layer was dried over $MgSO_4$ and filtered. Lastly, the residual reaction mixture was purified using silicagel column chromatography (eluent dichloromethane/ethyl acetate – 8/1 (v/v)) (yield: 60%)

^{1}H-NMR HEAm-EC ($CDCl_3$, 300 MHz), δ (ppm): 8.07 (s, 1H, imi-H), 7.36 (s, 1H, imi-H), 7.00 (s, 1H, imi-H), 4.42(q, 2H, *CH_2*-CH_3), 1.37 (t, 2H, CH_2-*CH_3*). ESI-MS $C_8H1_3NO_4$: calculated $[M + H]^+$, 188.2023 $[M + Na]^+$ 210.1842, $[M + K]^+$ 226.1582, found $[M + H]^+$ 188.0913, $[M + Na]^+$ 210.0735, $[M + K]^+$ 226.0479

2.5. Monomer hydrolysis kinetics

The monomer degradation kinetics were determined, based on a described protocol[16]. A 10 mM stock solution of HEAm-EC and HEAm-BC was prepared in DMSO. Next, 0.5 mL of the stock solution in DMSO was added to 4.5 mL of phosphate buffer (pH 7.4, 100 mM) or carbonate buffer (pH 10.0, 100 mM). The hydrolysis reactions were conducted at 37 °C in triplicate. At various time points, samples (50 µl) were drawn from the mixture and diluted with 950 µl phosphate buffer (pH 4.4, 100 mM) to stop any further degradation. The samples were stored at 4 °C until they were analyzed by HPLC. As eluent ACN/H_20 40/60 was used to determine the hydrolysis rate of HEAm-EC and HEAm-BC, with a flow rate of 0.2 mL/min and a detection wavelenght of 207 nm. The degradation rate of HEAm-BC was estimated based on the calibration curve of the molar ratio of HEAm-BC and benzylalcohol. Degradation samples of HEAm-EC were spiked with benzyl alcohol as internal standard because ethanol could not be detected, which allowed similar data analysis.

2.6. Synthesis of pHEAm-EC/BC homopolymer.

For the homopolymerization of HEAm-EC and HEAm-BC by RAFT polymerization, HEAm-EC, (2.5 mmol, 0.468 g) respectively HEAm-BC (2.5 mmol, 0.623 g), 2-(butylthiocarbonothioylthio)propanoic acid (PABTC) (0.063 mmol, 14.9 mg) and AIBN (0.013 mmol, 2.05 mg) were dissolved in dry DMF (2M). A monomer/CTA/AIBN molar ratio of 40:1:0.2 was used. The reaction mixture was degassed with five freeze-pump-thaw cycles and the reaction was conducted at 70 °C for two hours under a vacuum atmosphere. The polymer was isolated by precipitation in cold diethyl ether, and subsequently dried under vacuum at room temperature. Monomer conversion was determined by ^{1}H-NMR and polydispersity of purified polymer was analyzed by SEC.

2.6. Synthesis of poly(HEAm)$_x$macroCTA

A macromolecular RAFT chain transfer agent (MacroCTA) was synthesized by RAFT homopolymerization of *N*-(2-hydroxyethy)acrylamide (HEAm). pHEAm$_{64}$ was synthesized by dissolving PABTC (0.267 mmol, 63.6 mg), 2,2'-azobisisobutyronitrile (AIBN, 0.027 mmol, 4.38 mg) and HEAm (20 mmol, 2.303 g) in *N*,*N*-dimethylformamide (DMF) to obtain a monomer concentration of 2.0 M and a monomer/CTA/initiator molar ratio of 75:1:0.1. The mixture was degassed by five freeze−pump−thaw cycles, and the reaction was performed at 70 °C for 2 h under vacuum. The obtained polymer was purified by triple precipitation in cold diethyl ether. After centrifugation, the residue was dried overnight under vacuum at room temperature. Finally, the polymer was dialyzed at 5 °C against distilled water (MWCO 3.5 kDa) for 3 days and recollected after lyophilization. The homopolymer was analyzed by SEC and ^{1}H-NMR. The conversion of HEAm was determined by comparing the integration areas of the vinyl protons of unreacted HEAm at 5.30 ppm and the methylene group at 4,20 ppm. A similar protocol was used for the synthesis of pHEAM$_{140}$, but with a monomer/CTA/initiator molar ratio of 200:1:0,1.

2.7. Synthesis of pHEAm-pHEAmEC & -BC block copolymers

pHEAm$_{64}$ and pHEAm$_{140}$ – macroCTA were used for the synthesis of 8 block copolymers with various chain lengths. The second block was either composed of HEAm-EC or HEAm-BC. Variations in chain length were obtained by changing the monomer/CTA/initiator molar ratio. For the synthesis of pHEAm$_{64}$-pHEAmEC$_{26}$, pHEAm$_{64}$ (0.038 mmol, 285 mg), AIBN (0.008 mmol,1.23 mg) and HEAm-EC (1.2 mmol, 225 mg) were dissolved in anhydrous DMF, with a final monomer concentration of 0.90 M and a monomer/CTA/initiator molar ratio of 32:1:0.2. The reaction mixture was degassed with five freeze-pump-thaw cycles and the reaction was conducted at 80 °C for two hours under a vacuum atmosphere. The polymer was isolated by precipitation in cold diethyl ether, and subsequently dried under vacuum at room temperature. Finally, the polymer was dialyzed at 5 °C against distilled water (MWCO 3.5 kDa) for 3 days and recollected after lyophilization. The block copolymer was analyzed by ^{1}H NMR and SEC.

2.8. Synthesis of PEG-pHEAm-EC & -BC block copolymers

Block copolymers of HEAm-EC/HEAm-BC and ethylene glycol were synthesized using a commercially available PEG-CTA (5 kDA). A monomer/CTA/AIBN ratio of 50:1:0.2 and 100:1:01 were used. PEG$_{5000}$, HEAm-EC/HEAm-BC and AIBN were dissolved in DMF and degassed by five freeze-pump-thaw cycles. After 2 hours at 80 °C and under a vacuum atmosphere, the reaction was stopped by precipitation in cold diethyl ether. After drying under vacuum at room temperature, the polymer was dialyzed (MWCO 3.5 kDa) against distilled water for 3 days and recollected after lyophilization. The block copolymers were analyzed by ^{1}H NMR and SEC.

2.9. Micelle preparation

Polymeric micelles of PEG$_x$-pHEAmEC$_y$ and pHEAm$_m$-pHEAmEC$_n$ were prepared by adding the polymers to PBS at a concentration of 5 mg/mL followed by sonication for 1 min to form micelles. PEG$_x$-pHEAmBC$_y$ micelles were obtained by a nanoprecipitation technique, which involved dissolving 5 mg block copolymers in 1 mL THF.[20] Next, this solution was added dropwise to PBS in a 1:1 ratio, while stirring. After evaporation of THF for 48 hours, nanoparticles were formed. pHEAm$_m$-pHEAmBC$_n$ micelles were prepared by a dialysis method, where the blockcopolymers were dissolved in DMSO and dialyzed against PBS to trigger micelle formation.

2.10. Transmittance measurement

The cloud point (CP) of pHEAm-EC was investigated by turbidimetric analysis. First the block copolymer was dissolved in ice-cold PBS at a concentration of 5 mg/mL. Turbidity of the solution was measured by the transmission at 600 nm through the sample vial as a function of the temperature while stirring. The sample was heated up from 5 to 40 °C with a heating rate of 1 °C/min. The cloud point was taken as the onset of the drop in transmittance in the turbidity curve.

2.11. Polymer hydrolysis

For monitoring the evolution of particle size during hydrolysis of the carbonate ester side chain moieties, $pHEAm_x$-$pHEAmEC_y/BC_z$ and PEG-$pHEAmEC_m/BC_n$ were dissolved at 5 mg/mL in an aqueous 0.1 M NaOH solution (pH 13). Subsequently, particle size and light scattering intensity were measured at 37 °C at 15 min intervals.

2.12. Critical Micelle Concentration (CMC)

Dilution series of the block copolymers in PBS were prepared with concentrations ranging from 0.001-1 mg/mL. Next, a stock solution of pyrene in acetone (1.8×10^{-2} M) was prepared and kept on ice to prevent evaporation of the acetone. The stock solution was then diluted (1/100) and also kept on ice. Finally, 6,67 µL of the latter pyrene solution was added to 2 mL of each polymer dilution in triplicate under stirring (pyrene concentration 6.0×10^{-7} M). The polymer dispersions were vigorously vortexed and incubated overnight to promote particle formation and evaporate acetone. Fluorescence excitation spectra were recorded at room temperature with an excitation wavelength of 390 nm and monitored from 300-360 nm. The CMC was determined based on the change in excitation intensity ratio at 338 and 333 nm in function of the polymer concentrations.[16,21]

2.13. Cell culture

SKOV-3 (human ovarian cancer cell line) cells were cultured in DMEM, supplemented with 10% FBS, 2 mM L-glutamine, 1 mM sodium pyruvate and antibiotics (50 units/mL penicillin and 50 µg/mL streptomycin). Cells were incubated at 37 °C in a controlled, sterile environment of 95% relative humidity and 5% CO2. SKOV-3 cells were used for all cell experiment.

2.14. *In* vitro cellular uptake

2.14.1. Encapsulation hydrophobic fluorescent dye.

For the encapsulation of a hydrophobic, fluorescent dye, Octadecyl Rhodamine B Chloride was used. Octadecyl Rhodamine B Chloride was loaded into the nanoparticles using a solvent displacement technique. A small amount (100 µL) of an ethanolic solution (0.05 mg/mL) was added to the block copolymer dispersions in PBS (10 mg/mL) under stirring. As a control, the same ethanolic solution was added to pure PBS, leading to precipitation of the hydrophobic dye. Formulations were stabilized overnight at room temperature to allow evaporation of ethanol. The excess dye was removed by membrane filtration (0.450 µm).

2.14.2. Confocal Microscopy

Cells were plated in WillCo Wells dishes at a density of $5*10^3$ cells per well and allowed to adhere overnight. Subsequently, cells were pulsed for 16 hours with micelles 5 µL of 10 mg/mL R18-labeled block

copolymers followed by washing with PBS and fixation with 4 % paraformaldehyde. Prior to imaging, cell nuclei were stained with Hoechst 33342 (according to manufacturer's protocol) and the cell membrane was stained with AlexaFluor488-conjugated phalloidin.

2.15. Drug loading

Paclitaxel-loaded micelles of PEG_x-$pHEAmEC_y$ and $pHEAm_m$-$pHEAmEC_n$ were prepared by first dissolving the polymers in cold PBS at a concentration of 10 mg/mL. Next, a 10 mg/mL solution of PTX in acetone was prepared, and 100 µL of this solution was added to 1 mL of the cold (5 °C) polymer solution followed by rapid heating to 50 °C and sonication to allow for micelle formation. The formulation was allowed to stabilize overnight at room temperature, with the lid kept open to enable evaporation of the acetone.

The encapsulation of paclitaxel into the PEG_x-$pHEAmBC_y$ micelles, was carried out using the nanoprecipitation method.[20] Therefore, 1 mg of paclitaxel and 10 mg of polymers were dissolved in 1 mL of THF en added drop wise to 1 ml PBS. After evaporation of THF for 48 hours, nanoparticles were formed.

$pHEAM_m$-$pHEAmBC_n$ loaded micelles were prepared by a dialysis method, where blockcopolymers (10 mg) and paclitaxel (1 mg) were dissolved in 1 mL DMSO and dialyzed against PBS to trigger micelle formation and drug loading.

Finally, the free drug was removed by filtration (0.450 µm) and the paclitaxel concentration loaded into the micelles was determined by UPLC analysis, similar to a described protocol.[16] For this 100 µL of the PTX loaded micelle dispersion was diluted with 900 µL acetonitrile and vortexed to destabilize the micelles and fully dissolve the drug. Next, this was centrifuged for 15 min. at 15000 g and 2 µL of the supernatans was injected. A calibration curve of PTX was prepared by dissolving PTX in acetonitrile in a concentration range of 2-100 µg/mL. PTX was measured at a wavelength of 227 nm and from the determined PTX concentration, encapsulation efficiency (EE) and loading capacity (LC) were calculated as follows:

$$EE = \frac{concentration\ of\ measured\ PTX}{concentration\ of\ added\ PTX}\ x\ 100\%$$

$$LC = \frac{concentration\ of\ measured\ PTX}{concentration\ of\ measured\ PTX + concentration\ of\ added\ polymer}\ x\ 100\%$$

2.16. *In vitro* cytotoxicity

In vitro cytotoxicity was determined using the MTT assay as described earlier.[22,11] SKOV-3 cells were pulsed with different concentrations of PTX loaded micelles and as control nanoparticle formulations Abraxane (Celgene) and Genexol-PM (Samyang Biopharmaceuticals) were used. The MTT stock solution was prepared by dissolving 100 mg MTT in 20 mL of PBS and subsequent membrane filtration (0.22 µm). Before use, the MTT stock solution was 5-fold diluted with culture medium.

SKOV-3 cells were seeded into 96-well titer plates (10000 cells per well, suspended in 200 µL of culture medium) and incubated overnight. Next, 50 µL of sample, DMSO (positive control = 0% viability) or PBS (negative control = 100% viability), was added to the cells, followed by 72 h of incubation. Subsequently, the medium was aspirated and the cells were washed with 200 µL of PBS. After aspiration, 100 µL of MTT working solution was added and the cells were incubated for 2.5 h. Finally, the MTT working solution was

aspirated and the formed purple formazan crystals were dissolved in 50 µL of DMSO. Absorbance was determined at 590 nm using an EnVision Multilabel plate reader. The absorbance of the positive control was used as a blank and therefore subtracted from all values. The dilution series, positive and negative control were added to the wells in triplicate (n=3). Cell viability (%) was calculated according to the equation below.

$$cell\ viability = \frac{Abs\ (sample) - Abs\ (+control)}{Abs\ (-control) - Abs\ (+control)}\ x\ 100\%$$

3. Results and discussion

3.1 Monomer synthesis

HEAm-EC and HEAm-BC were synthesized by modifying HEAm with an ethyl/benzyl group via a carbonate ester (**FIgure 1**). Our previously reported route for the synthesis of HPMA-EC[11] involved activation of the hydroxyl group of HPMA with 1,1-carbonyldiimidazole (CDI) followed by a purification (extraction) step and subsequent reaction with a large excess of ethanol, affording the formation of a carbonate esters between the propylmethacrylamide moiety and the ethyl moiety. However, when this route was transposed to acrylamides, we faced extremely poor reaction yields due to Michael addition between the acrylamide moiety and the imidazole by-product that is formed during both reaction steps. Therefore, a crucial amendment to our previously reported synthesis was to first activated the hydroxyl group of ethanol/benzylalcohol, with (CDI) followed by a substitution reaction with HEAm, yielding 2-acrylamidoethyl ethyl carbonate (HEAm-EC) and 2-acrylamidoethyl benzyl carbonate (HEAm-BC) respectively (**Figure 1**). In both these reaction steps, the formed imidazole acts as a catalyst, and did not require the use of an additional base catalyst. By opting for this synthesis route, Michael addition is reduced between the α,β unsaturated carbonyl moiety of HEAm and imidazole, and affords yields up to 60 % for both monomers. ^{1}H-NMR and MS analysis of the synthesized monomers are shown in **Figure S1-S4**.

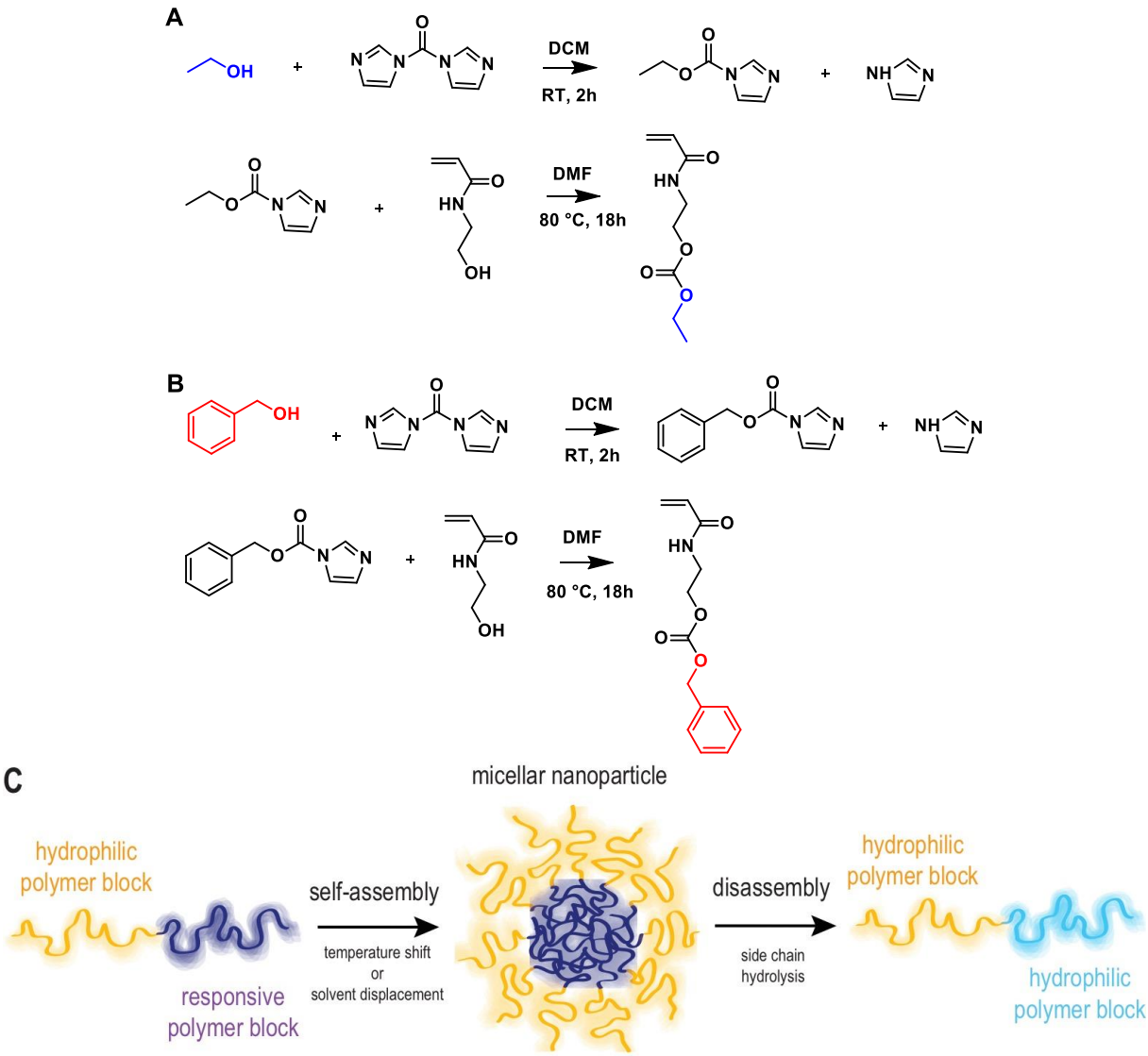

FIGURE 1: Synthesis of (A) HEAm-EC and (B) HEAm-BC. (C) Schematic representation of responsive block copolymer micelles.

3.2. Monomer degradation kinetics

The degradation kinetics of HEAm-EC and HEAm-BC were studied at pH 7.4, 9 and 10 at 37 °C by HPLC. The pH of 7.4 is representative of the physiological conditions and pH values of 9 and 10 were used to accelerate hydrolysis rate of the carbonate ester. Hydrolysis of the carbonate ester moiety results in liberation of CO_2 and ethanol or benzyl alcohol, respectively. Whereas benzyl alcohol could be readily detected by HPLC, allowing to take the ratio of benzyl alcohol to HEAm-BC, ethanol could not be detected and therefore HEAm-EC degradation samples were spiked with benzyl alcohol as internal standard which allowed similar data analysis as for HEAm-BC.

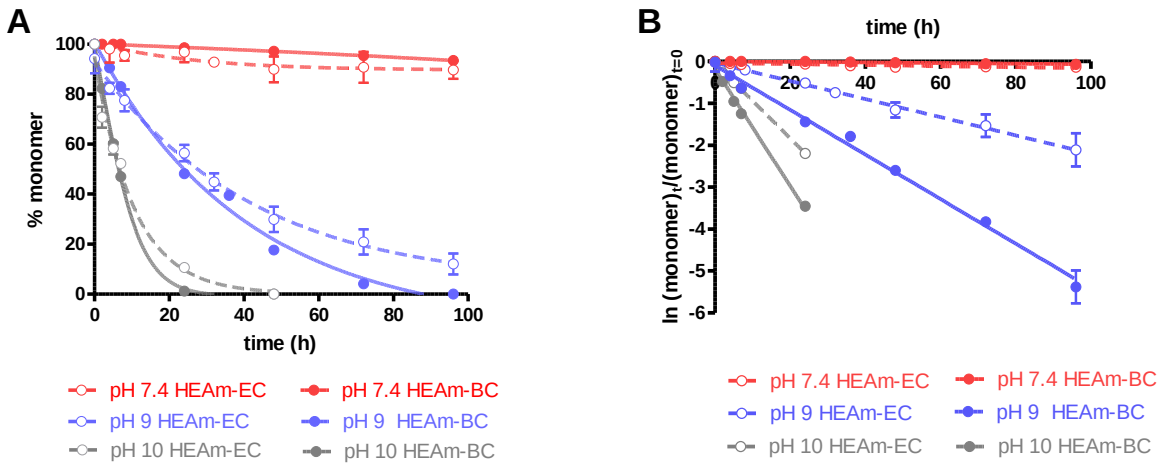

FIGURE 2: A) Hydrolysis of HEAm-EC and HEAm-BC at pH 7.4, 9 and 10. (n=3) B) First order kinetics of monomer hydrolysis with –d(monomer)/dt = k * monomer, which leads to ln((monomer)$_t$/(monomer)$_{t=0}$) = -k * t and (monomer)$_t$ = (monomer)$_{t=0}$* e $^{(-kt)}$; k: rate constant for hydrolysis; half-life $t_{1/2}$ = ln2 / k

For both HEAm-EC and HEAm-BC, the rates of hydrolysis were similar and followed for each pH first order kinetics. The calculated rate constants and half-lives are listed in the adjacent **Table 1.** Hydrolysis was strongly affected by the pH of the medium with full hydrolysis of both monomers occurring in less than 2 days at pH 10, whereas about a week was required to fully degrade at pH 9 and very slow hydrolysis was measured at pH 7.4.

Table 1: The calculated first-order reaction rate constants (k) and half lives $t_{(1/2)}$ at 37 °C and pH 7.4, 9 and 10

pH	$k_{HEAm-BC}$ (h^{-1})	$t_{(1/2)HEAm-BC}$ (h)	$k_{HEAm-EC}$ (h^{-1})	$t_{(1/2)HEAm-EC}$ (h)
7.4	(74 ± 4) *10^{-5}	(9.3 ± 0.8)*10^2	0.0011 ± 0.0003	(5.8± 2) *10^2
9	0.053 ± 0.001	13 ± 0.5	0.022 ± 0.001	32 ± 2
10	0.14 ± 0.004	5.0 ± 0.2	0.089 ± 0.002	7.8 ± 0.2

3.3. RAFT polymerization

First we verified that HEAm-EC and HEAm-BC could be polymerized by RAFT. To this end, 2-(butylthiocarbonothioylthio)propanoic acid (PABTC) was used as chain transfer agent (CTA) and AIBN as radical initiator. Anhydrous DMF was used as solvent to avoid hydrolysis of the carbonate esters. Size exclusion chromatography (SEC) analysis of the polymers showed a low dispersity (1.09 for both pHEAm-EC_{19} as pHEAm-BC_{33}) and ^{1}H-NMR analysis indicated the experimental degree of polymerization (DP) to

correspond well to the theoretical DP **(Table 2).** Taken together, these findings demonstrate that both HEAm-EC and HEAm-BC can be successfully be polymerized by RAFT and yield well-defined polymers.

Table 2: Compositional data of the synthesized polymers

	Monomer	CTA	M:CTA	Time (min.)	Conversion (%)[a]	DP[a]	Mn[a] (kDa)	Mn[b] (kDa)	Đ[b]	Tcp (°C)
pHEAmEC$_{19}$	HEAm-EC	PABTC	40:1	120	48	19	3.8	4.3	1.09	16
pHEAmBC$_{33}$	HEAm-BC	PABTC	40:1	120	83	33	8.5	8.6	1.09	/

[a]Calculated based on ^{1}H NMR spectroscopy data. [b]Determined by SEC in DMAc using PMMA for calibration.

The thermo-responsive properties of pHEAm-EC$_{19}$ were measured by turbidimetry at a polymer concentration of 5 mg/mL in phosphate buffered saline (PBS) (pH 7.4; 0.15 M NaCl). Samples were heated from 5 °C to 40 °C with a heating rate of 1 °C/min. The cloud point temperature (T_{cp}: i.e. the temperature at which the polymer precipitates from solution due to an entropically-driven coil-to-globule transformation) was determined to be 16 °C as evidenced by the drop in transmittance at 16 °C, which indicates phase separation. **(Figure 3).** The more hydrophobic pHEAMBC$_{33}$ even at low temperature does not dissolve in water and therefore does not have LCST properties.

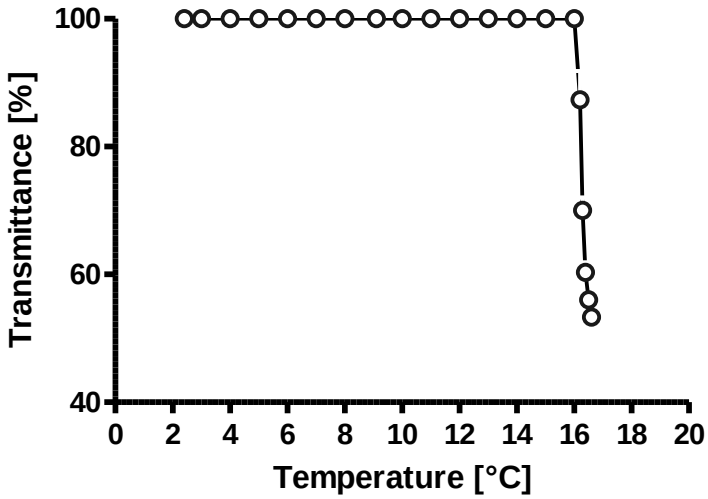

FIGURE 3: Transmittance versus temperature plot of pHEAm-EC$_{19}$

3.4. Block copolymer synthesis

Next, we synthesized amphiphilic block copolymers with poly(HEAm-EC), respectively poly(HEAm-BC), serving as hydrophobic block. As hydrophilic block, two different types of polymers were evaluated, i.e. poly(*N*-(2-hydroxyethyl)acrylamide) (poly(HEAm)) and poly(ethylene glycol) (PEG). PEG is a well-known stealth polymer and PEG with a molecular weights between 2-10 kDa, are often used as hydrophilic shell to provide colloid stability, evade opsonization by the reticuloendothelial system (RES) and hence

increase circulation half-life of nanomedicines.[23,24,25] Poly(HEAm) has been less studied, but also possesses hydrophilicity and likely similar behavior as poly(HPMA) which is also known for its stealth properties[26–28]

For the synthesis of a poly(HEAm) macro-CTA, we aimed at 2 different DPs, i.e. 75 and 200. A conversion of 85% and 70% was determined by ^{1}H-NMR, which correspond to a final theoretical DP of 64 and 140 respectively and a corresponding molecular weight of 7.6 and 16.4 kDa. SEC traces reveal a low dispersity (Đ) of 1.08 for poly(HEAm)$_{64}$ and 1.10 for poly(HEAm)$_{140}$, with a number average molecular weight (M_n) of 15.7 kDa and 23.5 kDa respectively. **(Table 3)**

Next, the poly(HEAm)$_x$-macroCTA's were extended with different block lengths of the HEAm-EC, respectively HEAm-BC. The properties of the resulting block polymers are listed in **Table 3**. According to ^{1}H-NMR, conversions between 70-91% were obtained for the block copolymers after a reaction time of 2h. SEC-traces (**Figure 4**) of the block copolymers show a shift to higher molecular weight values in comparison to the corresponding macro-CTAs, which confirm successful block copolymer formation. The dispersities of the polymers were low (< 1.2), except for the block copolymers based on the pHEAm$_{140}$-macroCTA, which were however still below 1.7. This can most likely be ascribed to the high DP of pHEAm$_{140}$-macroCTA, which results in sub-optimal chain extension and limited control over the polymerization.

For the synthesis of PEG-based block copolymers, we used a commercially available PEG macroCTA, i.e. poly(ethylene glycol) methyl ether 2-(dodecylthiocarbonothioylthio)-2-methylpropionate, with an average molecular weight of 5 kDa. The PEG macroCTA was extended with HEAm-EC, respectively HEAm-BC, aiming at a DP of 50 and 100. M_n and Đ were measured by SEC and are listed in **Table 3**. SEC traces for all polymers show residual homopolymer of unconverted PEG-CTA. We ascribe the presence of unreacted macroCTA rather to the poor quality of the commercial source rather than poor control over the RAFT block copolymerization. To correct for the fraction of unreacted CTA, peak deconvolution was applied to the SEC data and the experimental DP was recalculated based on the conversion and the fraction of unreacted macroCTA. These values are also listed in **Table 3**.

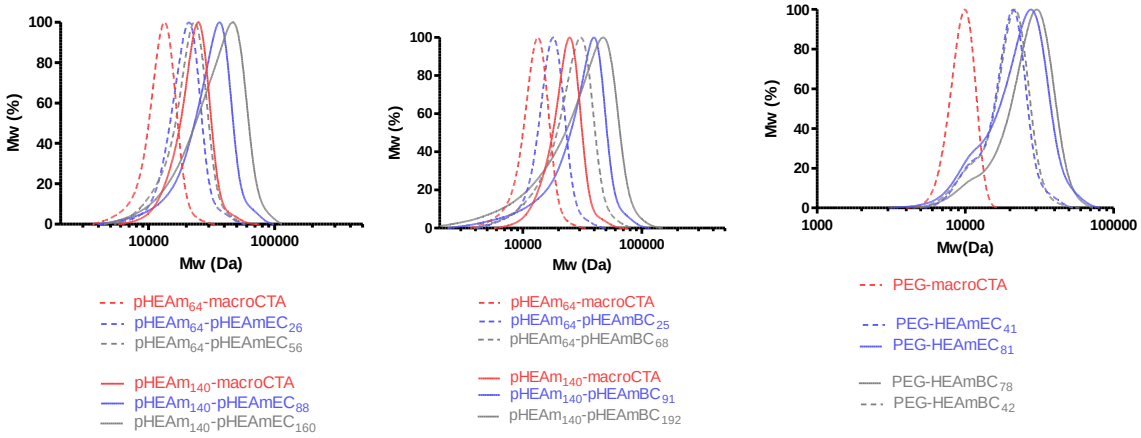

Figure 4: SEC traces of polymers before and after chain extension of the pHEAm$_x$- en PEG-macroCTA with HEAm-EC/HEAm-BC

TABLE 3: Compositional data for the synthesized polymers

(macro)CTA	Monomer (M)	M/CTA/AIBN	Conversion (%)	DP	M_{nSEC} (kDa)	Mntheo* (kDa)	Đ	Hydrophilic /hydrophobic ratio
PABTC-CTA	HEAm	75/1/0.2	85	64	15.7	7.6	1.08	/
	HEAm	200/1/0.2	70	140	23.5	16.4	1.10	/
Poly(HEAm)$_{64}$	HEAm-EC	32/1/0.2	81	26	18.2	12.5	1.11	0.41
		80/1/0.2	70	56	19.0	18.1	1.13	0.88
	HEAm-BC	32/1/0.2	78	25	15.9	13.8	1.11	0.39
		80/1/0.2	85	68	21.8	24.6	1.23	1.063
Poly(HEAm)$_{140}$	HEAm-EC	100/1/0.2	88	88	31.9	32.7	1.22	0.63
		200/1/0.2	80	160	37.2	46.3	1.31	1.14
	HEAm-BC	100/1/0.2	91	91	32.9	39.1	1.39	0.65
		200/1/0.2	86	172	35.6	59.3	1.67	1.23
PEG$_{5000}$	HEAm-EC	50/1/0.2	82	41	19.7	12.7	1.13	0.80
		100/1/0.2	81	81	19.8	20.2	1.24	1.50
	HEAm-BC	50/1/0.2	84	42	17.6	15.5	1.14	0.78
		100/1/0.2	78	78	27.6	24.4	1.20	1.44

* Calculated by ^{1}H-NMR

3.5. Self-assembly behavior in aqueous medium

Next we aimed at investigating the influence of different chain lengths of the hydrophobic block on the self-assembly behavior of the block copolymers in aqueous medium. For the latter, different protocols were used due to the different solubility of the respective block copolymers. pHEAm-EC, which exhibits LCST behavior, allows for self-assembly by rapid heating in phosphate buffered saline (PBS; pH 7.4, 150 mM NaCl) from below to above the cloud point temperature. This method has been described previously for self-assembly of thermoresponsive block copolymers by Soga et al.[29] Due to hydrophobicity of pHEAm-BC, self-assembly was performed by solvent displacement (from THF or DMSO into PBS, depending on the solubility of the hydrophilic block) for both PEG_x-pHEAm-BC_y and $pHEAm_m$-pHEAmBC_n. Subsequently, particle size was measured by dynamic light scattering (DLS) at 25 °C. Volume size distributions are shown in **Figure 5**. From these data, it can be concluded that all block polymers self-assemble into micellar nanoparticles with sizes between 10-100 nm and with low dispersity (<0.4) **Table SI1**. Nanoparticles within this size range are considered to be the ideal for long circulation in the bloodstream and diffusion into tumor tissue.[30] Furthermore, an increase in particle size was observed with increasing hydrophobic content. However, we also observed that a too elevated HEAm-BC content did not allow for the assembly of well-defined structures as observed by a multimodal size distribution of block copolymers with a HEAm-BC DP of 192.

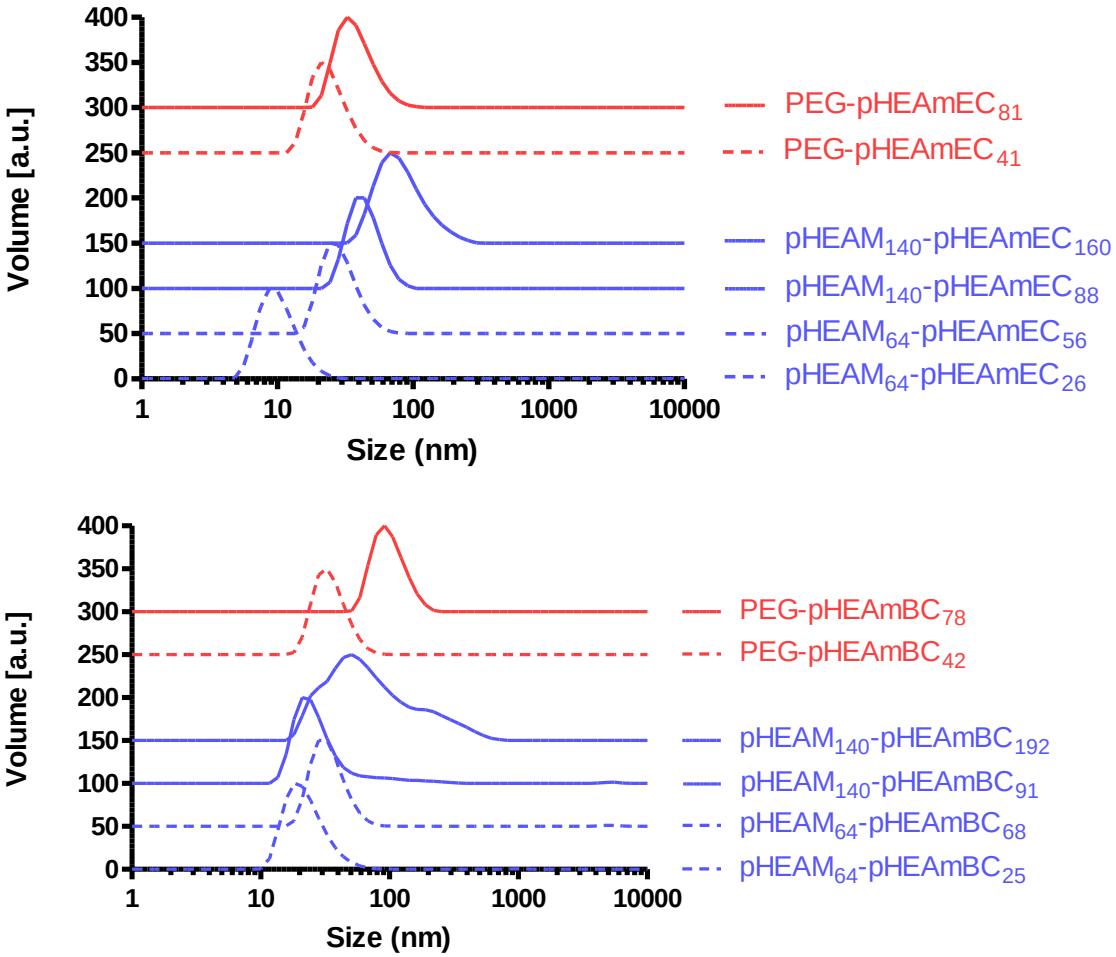

FIGURE 5: Volume size distribution histograms of the synthesized polymers measured by DLS.

3.6. Polymer hydrolysis

As described in section 3.2 the monomers HEAm-EC and HEAM-BC are degradable due to hydrolysis of the carbonate ester side chains. Therefore, block copolymer micelles based on these monomers should be converted into fully hydrophilic polymers upon prolonged exposure to aqueous medium. Hydrolysis of the carbonate esters liberates CO_2 and ethanol/benzylalcohol as benign byproducts. This will facilitate renal clearance of the resulting polymers, providing their molecular weight is below 40 kDa[31], which is the case in our present study, thereby preventing long-term accumulation in the body. To investigate hydrolysis-triggered disassembly of the micelles, the block polymers were dissolved in 0.1 M NaOH (pH 13, *i.e.* accelerated degradation conditions) at 37 °C, and analyzed by DLS. **Figure 6** shows a decrease in particle sizes upon exposure of the polymers under basic conditions, which indicates the formation of soluble unimers. In accordance to the hydrolysis rate of the monomers at physiological conditions, slow degradation rates at neutral pH are expected[29].

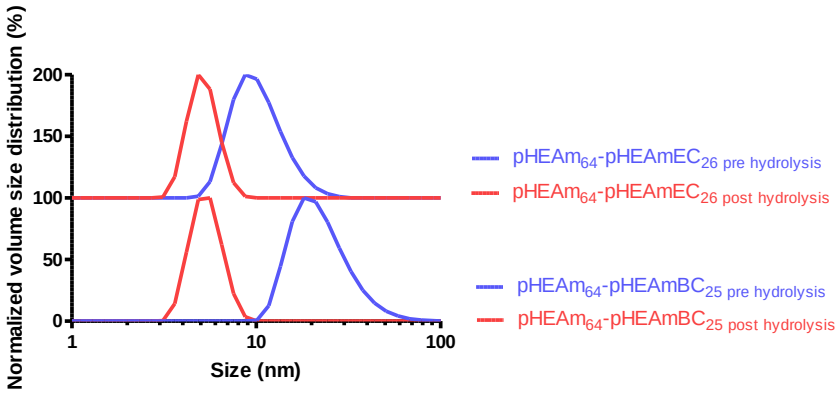

FIGURE 6. Hydrolysis of $_{p}$HEAm$_{64}$-$_{p}$HEAmEC$_{26}$ and $_{p}$HEAm$_{64}$-pHEAmBC$_{25}$ in 0.1 M NaOH (pH 13), monitored by DLS

3.7. Critical Micelle Concentration (CMC)

The CMC of the polymers was determined using pyrene as fluorescent probe in PBS at 37°C according to a previously published method.[22] **Figure 7** depicts the excitation intensity ratio of pyrene at 338 nm (I_3) and 333 nm (I_1) versus the polymer concentration. The onset of aggregate formation is shown by an abrupt change in the slope of the tangent curves with increasing polymer concentration. The CMC is used to characterize the thermodynamic stability of the polymeric micelles upon dilution in the bloodstream. CMC is among other things dependent on the nature and length of the hydrophobic block and length of hydrophilic block.[32] The CMC values of HEAm-BC-based block copolymers were found to be lower than HEAm-EC-based block copolymers. **(Table 4)** Most likely this is due to hydrophobicity and stacking interactions of the aromatic benzyl group, which suggests good stability. Moreover, a further decrease of CMC is observed with increasing length of the hydrophobic EC/BC segment. However, except for pHEAm$_{64}$-pHEAmBC$_{25}$, no difference in CMC values is observed for the polymers with distinct HEAm-BC block lengths. This can most likely be ascribed to the detection limit of the pyrene assay as at very low polymer concentrations, a relatively larger fraction of the pyrene probe will tend to distribute into the aqueous phase instead of the micelle core. Moreover, we observed that the nature of the hydrophilic block also has a significant influence on CMC. Block copolymer micelles based on PEG, show a much lower CMC and hence formed more stable nanoparticles in comparison to their pHEAm-counterparts. At present we do not have a clear explanation for this phenomenon which could be due to differences in polarity, flexibility, etc. This is subject of our ongoing investigations.

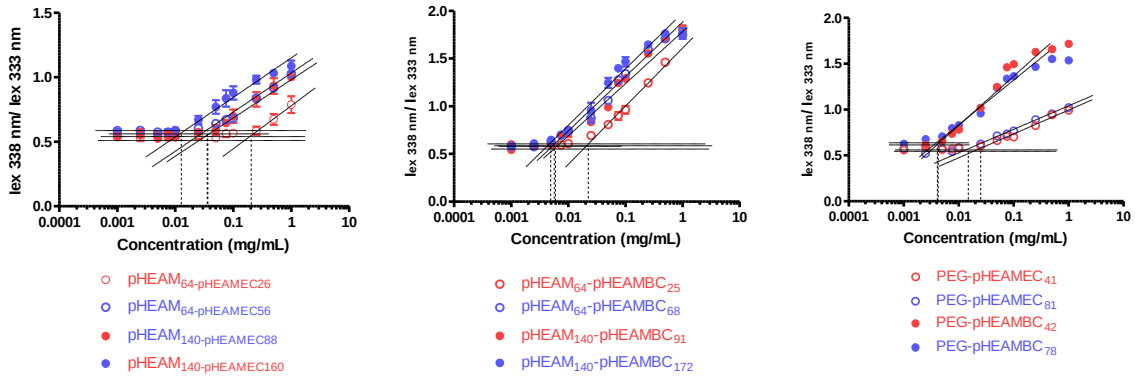

FIGURE 7: Intensity ratio of pyrene at 338 nm (I_3) and 333 nm (I_1) as a function of polymer concentration, determined by fluorescence spectrophotometry at 37 °C (n=3)

TABLE 4. Numeric values for CMC of different polymers (n= 3)

$Polymer_{HEAm-EC}$	CMC (mg/mL)	$Polymer_{HEAm-BC}$	CMC (mg/mL)
$pHEAm_{64}$-$pHEAmEC_{26}$	0.081 ± 0.03	**$pHEAm_{64}$-$pHEAmBC_{25}$**	0.024 ± 0.002
$pHEAm_{64}$-$pHEAmEC_{56}$	0.031 ± 0.002	**$pHEAm_{64}$-$pHEAmBC_{68}$**	0.0047 ± 0.0004
$pHEAm_{140}$-$pHEAmEC_{88}$	0.028 ± 0.003	**$pHEAm_{140}$-$pHEAmBC_{91}$**	0.0051 ± 0.0004
$pHEAm_{140}$-$pHEAmEC_{160}$	0.0075 ± 0.0002	**$pHEAm_{140}$-$pHEAmBC_{172}$**	0.0041 ± 0.0005
PEG-$pHEAmEC_{41}$	0.023 ± 0.004	**PEG-$pHEAmBC_{41}$**	0.0036 ± 0.0006
PEG-$pHEAmEC_{81}$	0.0096 ± 0.003	**PEG-$pHEAmBC_{78}$**	0.0033 ± 0.0003

3.8. *In vitro* cellular uptake

Rhodamine B octadecyl chloride (R18), a model red fluorescent dye, was used to investigate whether the nanoparticles are able to enhance intracellular delivery of a hydrophobic payload. For this purpose we used the SKOV-3 human ovarian cancer cell line. Block copolymers micelles were loaded with the dye by solvent displacement from ethanol into PBS. When adding the dye to PBS, immediate precipitation occurred. However, when the dye was added to a micelle formulation, no precipitation occurred, demonstrating that this hydrophobic dye was solubilized in the hydrophobic core of the micelles.

Confocal microscopy was performed to determine whether the fluorescent payload was internalized by the cells or merely bound to the cell membrane. After pulsing with micelles, cells were fixated and stained with Hoechst and AlexaFluor488-conjugated phalloidin to visualize the cell nuclei and cell membrane, respectively. The confocal images in **Figure 8** show that except for the blank, all micelle formulations afford intracellular delivery of the hydrophobic R18 payload.

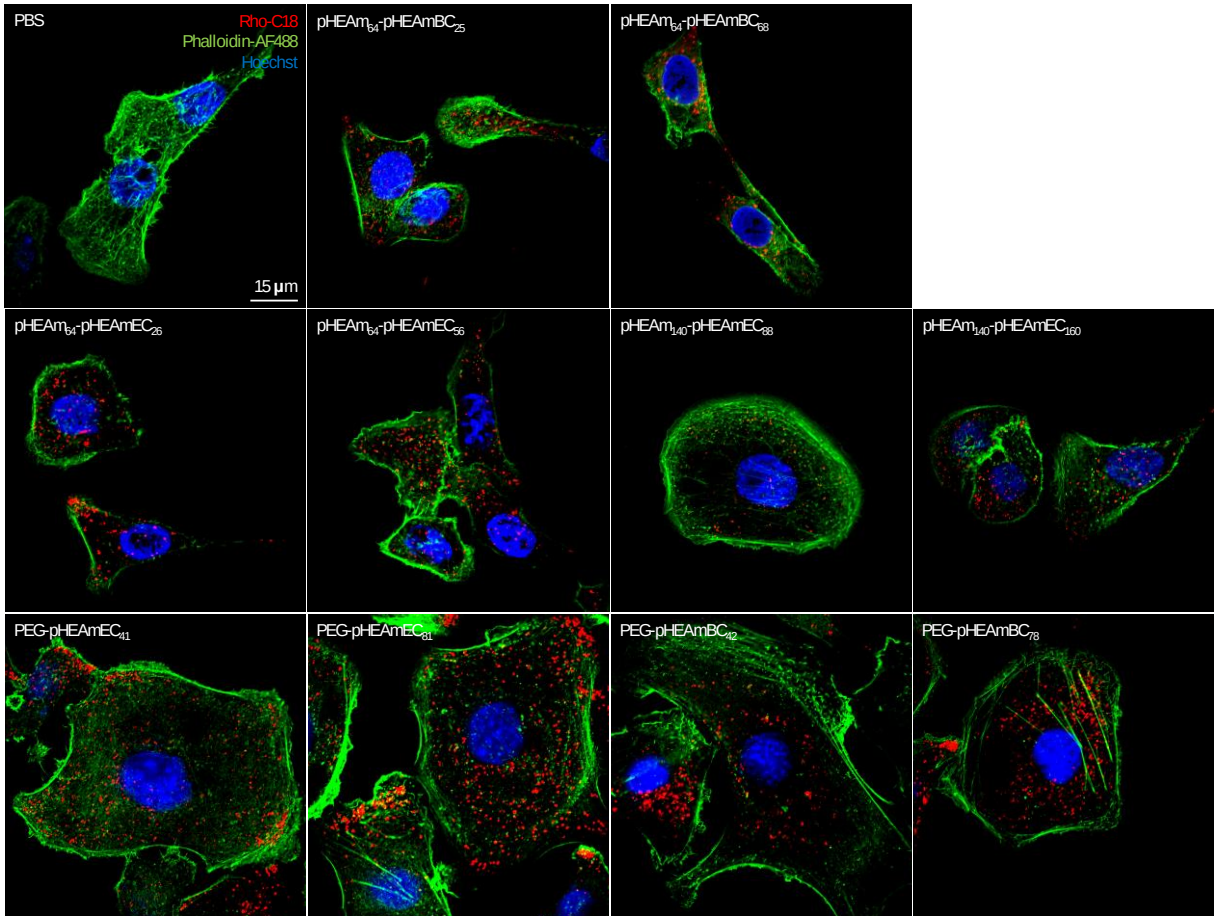

FIGURE 8: Confocal microscopy image of SKOV-3 human ovarian cells pulsed for 16h with rhodamine loaded micelles (red fluorescence). Cell nuclei were stained in blue by Hoechst, and cell membrane was stained in green by AlexaFluor488 conjugated phalloidin.

3.9. Drug formulation

To investigate the potential of the block copolymers for solubilization of hydrophobic drug molecules, we opted for paclitaxel. Paclitaxel (PTX) is a potent anti-tumor agent, used for various malignancies among them ovarian and breast cancer.[33] However, a major hurdle is the poor aqueous solubility (0.3 µg/mL) which hampers the delivery of therapeutic dosages. Taxol was the first clinical PTX formulation and comprise a mixture of Cremophor El (CrEL) and dehydrated ethanol (50:50). CrEL, a non-ionic surfactant, elicits a range of side effects, including serious hypersensitivity reactions, nephro-and neurotoxicity, which are dose limiting and require clinical intervention. [33–36] Therefore, alternative formulations for PTX were investigated and this led to the approval of Abraxane, a nanoparticle formulation of human serum albumin and PTX.[37] The first approved polymeric micelle formulation of PTX is Genexol-PM that consist of an amphiphilic block copolymer of PEG en poly(D,L) lactide (PLA). [38] It is approved in South Korea and is undergoing clinical trials in the US. There are several other polymeric micelles that are developed and/or progressing in clinical trials, which show the potential as drug delivery system for the effective therapy of cancer and non-cancerous diseases.[22,39 ,40,41,42]

The loading procedure of PTX in the micelles is described in section 2.15. The encapsulation efficiency (EE) and loading capacity (LC) were determined by UPLC (**Figure 9**). These data show that by increasing the core block length, both the EE and LC increase. Moreover, a higher encapsulation of the drug is

observed in the micelles with HEAm-BC as core-forming block, which can be explained by higher polymer-drug compatibility due to strong Π-Π interactions between the aromatic groups of PTX and the HEAm-BC block. Also, micelles based on PEG, show more promising results, i.e. higher LC en EE in comparison to pHEAm-based micelles. These findings can be linked to the lower CMC values measured form PEG-based micelles (**Figure 7**), which suggest that a more stable hydrophobic core, as formed by PEG-based micelles, is favorable for encapsulation of PTX.

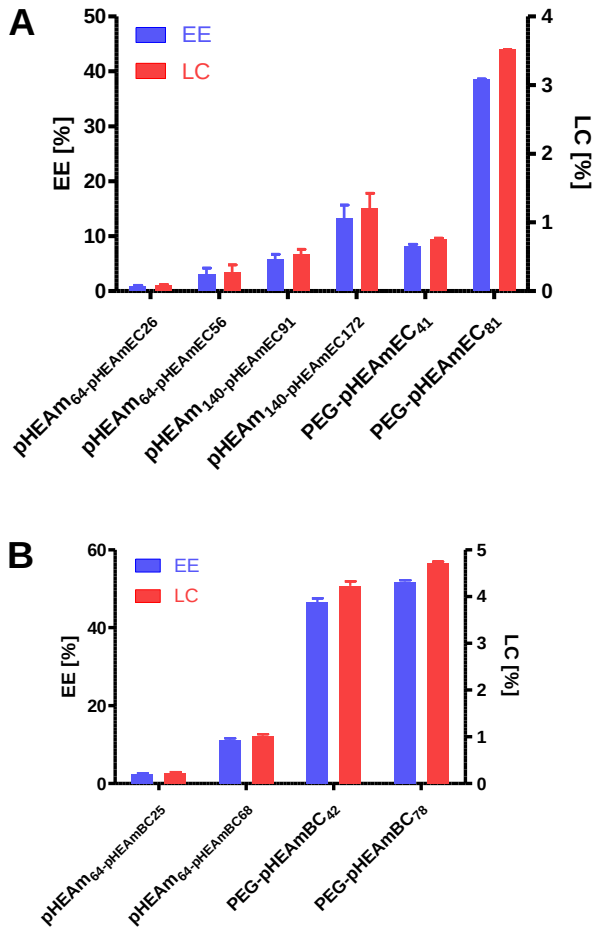

Figure 9: Calculated encapsulation efficiency (EE) and loading capacity (LC) of PTX-loaded micelles.

3.10. *In vitro* cytotoxicity

The *in vitro* cytotoxicity of PTX-loaded – and empty micelles was investigated by MTT-assay on SKOV-3 cells. Abraxane, an albumin-bound formulation of paclitaxel and Genexol-PM, a PTX-loaded PEG–poly-(lactide) block copolymer micelle formulation, were used as control formulations. After 72 hours of incubation, the inhibitory effect of PTX on cell growth was measured. As shown in **Figure 10A**, no intrinsic toxicity is observed for all empty micelles within the tested concentration range (up to 1 mg/mL) which indicates good cytocompatibility of the block copolymers within the experimental window. PTX-loaded micelles show a dose-dependent increase in cytotoxicity, comparable to Abraxane and Genexol-PM (**Figure 10B**). The cytotoxic effect of PTX will most likely be the result of the dilution effect, diffusion of the drug out of the micelles (as at lower PTX concentration the polymer concentration will be below the CMC (**Table S2**)) and binding to other hydrophobic binding sites in the cell culture medium or within the

cell. To a much lower extent, degradation of the polymers could also contribute to the cytotoxic effect of PTX.

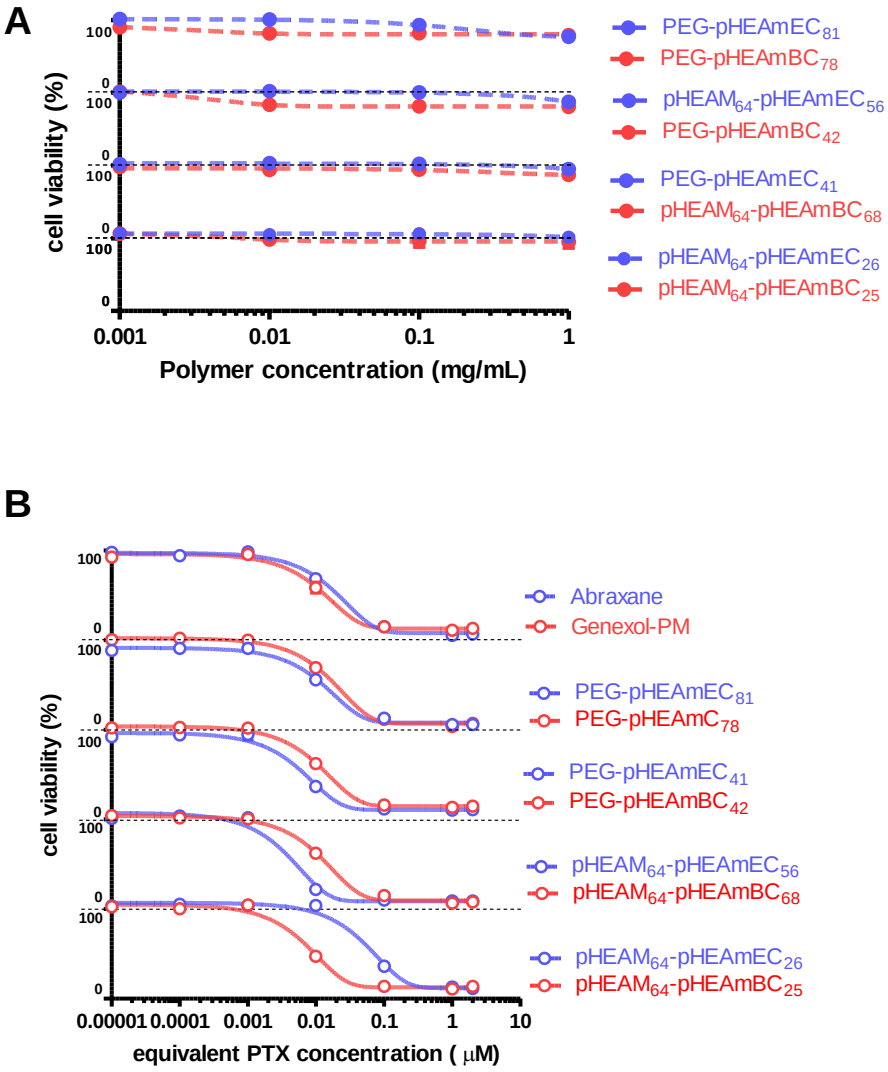

Figure 10. (A) *In vitro* cytotoxicity of unloaded micelles on SKOV-3 cells after 72 h of incubation (n=3). (B) *In vitro* cytotoxicity of PTX-loaded micelles on SKOV-3 cells after 72 h of incubation (n=3). Abraxane and Genexol PM were used as control nanoformulations.

4. Conclusions

In this paper we introduced a novel class of degradable polyacrylamides based on the hydrophobic modification of the readily available hydrophilic *N*-(2-hydroxyethyl)acrylamide (HEAm). The pending hydroxyl group of HEAm was modified with either an ethyl or benzyl group via a hydrolytically sensitive carbonate ester. Degradation of the carbonate ester moieties results in the release of CO_2 and ethanol/benzylalcohol as benign byproducts. Efficient RAFT polymerization of these monomers was observed and a library of well-defined block polymers with different degrees of polymerization (DP) was synthesized. The block copolymers formed micellar nanoparticles (10-100 nm) in PBS and could

efficiently solubilize hydrophobic compounds. The introduction of a benzyl carbonate ester side chain increased micellar stability and drug loading capacity. Moreover, PEG showed the most optimal performance in terms of micellar stability and drug loading capacity as well. Confocal microscopy showed that the micelles can efficiently deliver a hydrophobic payload to *in vitro* cultured cancer cells. Finally we also demonstrated efficient formulation of paclitaxel with an *in vitro* cancer cell killing performance comparable or even better than two commercial available PTX nanoformulations. In our ongoing research endeavours, the versatility of the RAFT approach will be further explored in the direction of core crosslinking and covalent drug ligation to ensure stability in the blood stream and in the direction of active targeting using small molecule ligand functionalized RAFT chain transfer agents.

References

(1) Yokoyama, M. Polymeric micelles as drug carriers: their lights and shadows. *J Drug Target* **2014**, *22* (7), 576–583 DOI: 10.3109/1061186X.2014.934688.

(2) Gaal, E. V. B. van; Crommelin, aan J. A. Polymeric Micelles. In *Non-Biological Complex Drugs,*; 2015; pp 11–76.

(3) Deng, C.; Jiang, Y.; Cheng, R.; Meng, F.; Zhong, Z. Biodegradable polymeric micelles for targeted and controlled anticancer drug delivery: Promises, progress and prospects. *Nano Today* **2012**, *7* (5), 467–480 DOI: 10.1016/j.nantod.2012.08.005.

(4) Cabral, H.; Kataoka, K. Progress of drug-loaded polymeric micelles into clinical studies. *J. Control. Release* **2014**, *190*, 465–476 DOI: 10.1016/j.jconrel.2014.06.042.

(5) Vanparijs, N.; Nuhn, L.; De Geest, B. G. Transiently thermoresponsive polymers and their applications in biomedicine. *Chem. Soc. Rev.* **2017**, *46*, 1193–1239 DOI: 10.1039/C6CS00748A.

(6) Ahmad, Z.; Shah, A.; Siddiq, M.; Kraatz, H.-B. Polymeric micelles as drug delivery vehicles. *RSC Adv.* **2014**, *4* (33), 17028–17038 DOI: 10.1039/C3RA47370H.

(7) Matsumura, Y.; Maeda, H. A new concept for macromolecular therapeutics in cnacer chemotherapy: mechanism of tumoritropic accumulatio of proteins and the antitumor agents Smancs. *Cancer Res.* **1986**, *46* (December), 6387–6392 DOI: 10.1021/bc100070g.

(8) Fang, J.; Nakamura, H.; Maeda, H. The EPR effect: Unique features of tumor blood vessels for drug delivery, factors involved, and limitations and augmentation of the effect. *Adv. Drug Deliv. Rev.* **2011**, *63* (3), 136–151 DOI: 10.1016/j.addr.2010.04.009.

(9) Maeda, H.; Wu, J.; Sawa, T.; Matsumura, Y.; Hori, K. Tumor vascular permeability and the EPR effect in macromolecular therapeutics: A review. *J. Control. Release* **2000**, *65* (1–2), 271–284 DOI: 10.1016/S0168-3659(99)00248-5.

(10) Maeda, H.; Nakamura, H.; Fang, J. The EPR effect for macromolecular drug delivery to solid tumors: Improvement of tumor uptake, lowering of systemic toxicity, and distinct tumor imaging in vivo. *Adv. Drug Deliv. Rev.* **2013**, *65* (1), 71–79 DOI: 10.1016/j.addr.2012.10.002.

(11) Kasmi, S.; Louage, B.; Nuhn, L.; Van Driessche, A.; Van Deun, J.; Karalic, I.; Risseeuw, M.; Van Calenbergh, S.; Hoogenboom, R.; De Rycke, R.; et al. Transiently responsive block copolymer micelles based on N-(2-hydroxypropyl)methacrylamide engineered with hydrolyzable ethylcarbonate side chains. *Biomacromolecules* **2016**, *17* (1), 119–127 DOI: 10.1021/acs.biomac.5b01252.

(12) Averick, S.; Mehl, R. A.; Das, S. R.; Matyjaszewski, K. Well-defined biohybrids using reversible-deactivation radical polymerization procedures. *J. Control. Release* **2015**, *205*, 45–57 DOI: 10.1016/j.jconrel.2014.11.030.

(13) Luo, K.; Yang, J.; Kopec□kova□, P.; Kopec□ek, J. Biodegradable Multiblock Poly[N -(2-hydroxypropyl)methacrylamide] via Reversible Addition−Fragmentation Chain Transfer Polymerization and Click Chemistry. *Macromolecules* **2011**, *44* (8), 2481–2488 DOI: 10.1021/ma102574e.

(14) Shi, Y.; Van Den Dungen, E. T. a; Klumperman, B.; Van Nostrum, C. F.; Hennink, W. E. Reversible addition-fragmentation chain transfer synthesis of a micelle-forming, structure reversible thermosensitive diblock copolymer based on the N-(2-hydroxy propyl) methacrylamide backbone. *ACS Macro Lett.* **2013**,

2 (5), 403–408 DOI: 10.1021/mz300662b.
(15) Hong, C. Y.; Pan, C. Y. Direct synthesis of biotinylated stimuli-responsive polymer and diblock copolymer by RAFT polymerization using biotinylated trithiocarbonate as RAFT agent. *Macromolecules* **2006**, *39* (10), 3517–3524 DOI: 10.1021/ma052593+.
(16) Shi, Y.; Van Steenbergen, M. J.; Teunissen, E. A.; Novo, L.; Gradmann, S.; Baldus, M.; Van Nostrum, C. F.; Hennink, W. E. Π-Π Stacking increases the stability and loading capacity of thermosensitive polymeric micelles for chemotherapeutic drugs. *Biomacromolecules* **2013**, *14* (6), 1826–1837 DOI: 10.1021/bm400234c.
(17) Shi, Y.; Van Der Meel, R.; Theek, B.; Oude Blenke, E.; Pieters, E. H. E.; Fens, M. H. A. M.; Ehling, J.; Schiffelers, R. M.; Storm, G.; Van Nostrum, C. F.; et al. Complete regression of xenograft tumors upon targeted delivery of paclitaxel via Π- Π stacking stabilized polymeric micelles. *ACS Nano* **2015**, *9* (4), 3740–3752 DOI: 10.1021/acsnano.5b00929.
(18) Ferguson, C. J.; Hughes, R. J.; Nguyen, D.; Pham, B. T. T.; Gilbert, R. G.; Serelis, A. K.; Such, C. H.; Hawkett, B. S. Ab Initio Emulsion Polymerization by RAFT-Controlled Self-Assembly §. *Macromolecules* **2005**, *38* (6), 2191–2204 DOI: 10.1021/ma048787r.
(19) Luten, J.; Akeroyd, N.; Funhoff, A.; Lok, M. C.; Talsma, H.; Hennink, W. E. Methacrylamide polymers with hydrolysis-sensitive cationic side groups as degradable gene carriers. *Bioconjug. Chem.* **2006**, *17* (4), 1077–1084 DOI: 10.1021/bc060068p.
(20) Fessi, H.; Puisieux, F.; Devissaguet, J. P.; Ammoury, N.; Benita, S. Nanocapsule formation by interfacial polymer deposition following solvent displacement. *Int. J. Pharm.* **1989**, *55* (1), 1–4 DOI: 10.1016/0378-5173(89)90281-0.
(21) Kalyanasundaram, K.; Thomas, J. . Environmental Effects on Vibronic Band Intensities in Pyrene Monomer Fluorescence and Their Application in Studies of Micellar Systems K. *J. Am. Chem. Soc.* **1977**, *99* (7), 2039–2044.
(22) Louage, B.; Zhang, Q.; Vanparijs, N.; Voorhaar, L.; Shi, Y.; Hennink, W. E.; Bocxlaer, J. Van; Hoogenboom, R.; De Geest, B. G. Degradable Ketal-Based Block Copolymer Nanoparticles for Anticancer Drug Delivery : A Systematic Evaluation. *Biomacromolecules* **2015**, *16* (1), 336–350.
(23) Knop, K.; Hoogenboom, R.; Fischer, D.; Schubert, U. S. Poly(ethylene glycol) in drug delivery: Pros and cons as well as potential alternatives. *Angew. Chemie - Int. Ed.* **2010**, *49* (36), 6288–6308 DOI: 10.1002/anie.200902672.
(24) Owens, D. E.; Peppas, N. a. Opsonization, biodistribution, and pharmacokinetics of polymeric nanoparticles. *Int. J. Pharm.* **2006**, *307* (1), 93–102 DOI: 10.1016/j.ijpharm.2005.10.010.
(25) Li, S. D.; Huang, L. Stealth nanoparticles: High density but sheddable PEG is a key for tumor targeting. *J. Control. Release* **2010**, *145* (3), 178–181 DOI: 10.1016/j.jconrel.2010.03.016.
(26) Talelli, M.; Rijcken, C. J. F.; van Nostrum, C. F.; Storm, G.; Hennink, W. E. Micelles based on HPMA copolymers. *Adv. Drug Deliv. Rev.* **2010**, *62* (2), 231–239 DOI: 10.1016/j.addr.2009.11.029.
(27) Kopeček, J.; Kopečková, P. HPMA copolymers: Origins, early developments, present, and future. *Adv. Drug Deliv. Rev.* **2010**, *62* (2), 122–149 DOI: 10.1016/j.addr.2009.10.004.
(28) Ulbrich, K.; Šubr, V. Structural and chemical aspects of HPMA copolymers as drug carriers. *Adv. Drug Deliv. Rev.* **2010**, *62* (2), 150–166 DOI: 10.1016/j.addr.2009.10.007.
(29) Soga, O.; van Nostrum, C. F.; Ramzi, A.; Visser, T.; Soulimani, F.; Frederik, P. M.; Bomans, P. H. H.; Hennink, W. E. Physicochemical Characterization of Degradable Thermosensitive Polymeric Micelles. *Langmuir* **2004**, *20* (21), 9388–9395 DOI: 10.1021/la048354h.
(30) Cabral, H.; Matsumoto, Y.; Mizuno, K.; Chen, Q.; Murakami, M.; Kimura, M.; Terada, Y.; Kano, M. R.; Miyazono, K.; Uesaka, M.; et al. Accumulation of sub-100 nm polymeric micelles in poorly permeable tumours depends on size. *Nat. Nanotechnol.* **2011**, *6* (12), 815–823 DOI: 10.1038/nnano.2011.166.
(31) Seymour, L. .; Duncan, R.; Strohalm, J.; Kopeček, J. Effect of molecular weight (mw) of N-(2-hydroxypropyl)methacrylamide copolymers on body distribution and rate of excretion after subcutaneous, intraperitoneal, and intravenous administration to rats L. *J. Biomed. Mater. Res.* **1987**, *21*, 1341–1358.
(32) Jones, M.; Leroux, J. Polymeric micellesea new generation of colloidal drug carriers. *Eur J PharmBiopharm* **1999**, *48*, 101–111.
(33) He, Z.; Wan, X.; Schulz, A.; Bludau, H.; Dobrovolskaia, M. A.; Stern, S. T.; Montgomery, S. A.; Yuan, H.; Li, Z.; Alakhova, D.; et al. A High Capacity Polymeric Micelle of Paclitaxel: Implication of High Dose Drug Therapy to Safety and In Vivo Anti-Cancer Activity. *Biomaterials* **2016**, *101*, 296–309 DOI: 10.1016/j.biomaterials.2016.06.002.This.

(34) Singla, A. K.; Garg, A.; Aggarwal, D. Paclitaxel and its formulations. *Int. J. Pharm.* **2002**, *235* (1–2), 179–192 DOI: 10.1016/S0378-5173(01)00986-3.
(35) Gelderblom, H.; Verweij, J.; Nooter, K.; Sparreboom, a. Cremophor EL: The drawbacks and advantages of vehicle selection for drug formulation. *Eur. J. Cancer* **2001**, *37* (13), 1590–1598 DOI: 10.1016/S0959-8049(01)00171-X.
(36) Panchagnula, R. Pharmaceutical aspects of paclitaxel. *Int. J. Pharm.* **1998**, *172* (1–2), 1–15 DOI: 10.1016/S0378-5173(98)00188-4.
(37) Green, M. R.; Manikhas, G. M.; Orlov, S.; Afanasyev, B.; Makhson, A. M.; Bhar, P.; Hawkins, M. J. Abraxane, a novel Cremophor-free, albumin-bound particle form of paclitaxel for the treatment of advanced non-small-cell lung cancer. *Ann. Oncol.* **2006**, *17* (8), 1263–1268 DOI: 10.1093/annonc/mdl104.
(38) Werner, M. E.; Cummings, N. D.; Sethi, M.; Wang, E. C.; Sukumar, R.; Moore, D. T.; Wang, A. Z. Preclinical evaluation of genexol-pm, a nanoparticle formulation of paclitaxel, as a novel radiosensitizer for the treatment of non-small cell lung cancer. *Int. J. Radiat. Oncol. Biol. Phys.* **2013**, *86* (3), 463–468 DOI: 10.1016/j.ijrobp.2013.02.009.
(39) Gothwal, A.; Khan, I.; Gupta, U. Polymeric Micelles: Recent Advancements in the Delivery of Anticancer Drugs. *Pharm. Res.* **2016**, *33* (1), 18–39 DOI: 10.1007/s11095-015-1784-1.
(40) Shi, J.; Kantoff, P. W.; Wooster, R.; Farokhzad, O. C. Cancer nanomedicine: progress, challenges and opportunities. *Nat. Rev. Cancer* **2017**, *17*, 20–37 DOI: 10.1038/nrc.2016.108.
(41) Louage, B.; Nuhn, L.; Risseeuw, M. D. P.; Vanparijs, N.; De Coen, R.; Karalic, I.; Van Calenbergh, S.; De Geest, B. G. Well-Defined Polymer-Paclitaxel Prodrugs by a Grafting-from-Drug Approach. *Angew. Chemie - Int. Ed.* **2016**, *55* (39), 11791–11796 DOI: 10.1002/anie.201605892.
(42) Zhang, Y.; Huang, Y.; Li, S. Polymeric Micelles: Nanocarriers for Cancer-Targeted Drug Delivery. *AAPS PharmSciTech* **2014**, *15* (4), 862–871 DOI: 10.1208/s12249-014-0113-z.

Supporting Information

Acrylamides with hydrolytically labile carbonate ester side chains as versatile building blocks for well-defined block copolymer micelles via RAFT polymerization

Sabah Kasmi,[a] Benoit Louage,[a] Lutz Nuhn,[a] Glenn Verstraete [a], Simon Van Herck [a], Mies J. van Steenbergen [b], Chris Vervaet;[a] Jean Paul Remon, *[a] Wim E. Hennink [b], Bruno G. De Geest,[a]**

[a] Department of Pharmaceutics, Ghent University, Ghent, Belgium

[b] Department of Pharmaceutics, Utrecht Institute for Pharmaceutical Sciences, Utrecht University, Utrecht, The Netherlands

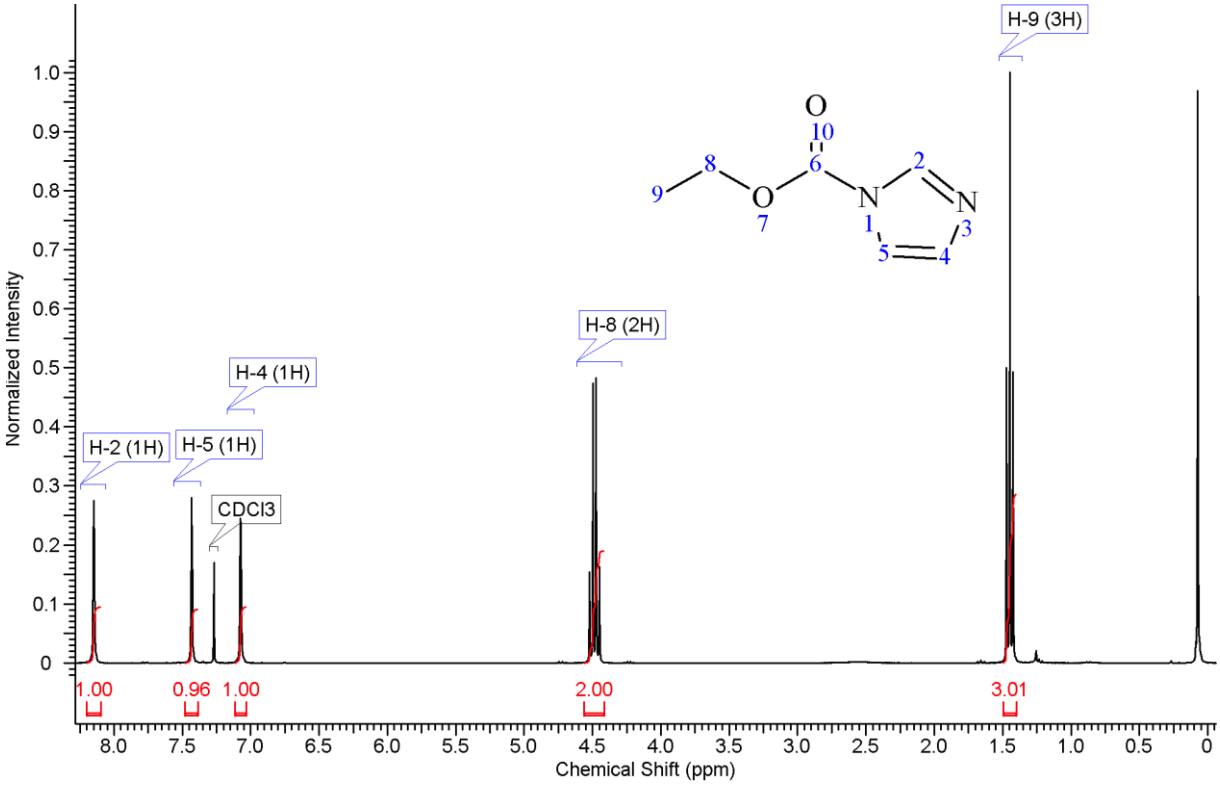

Figure S1. ^{1}H-NMR of CI-activated ethanol

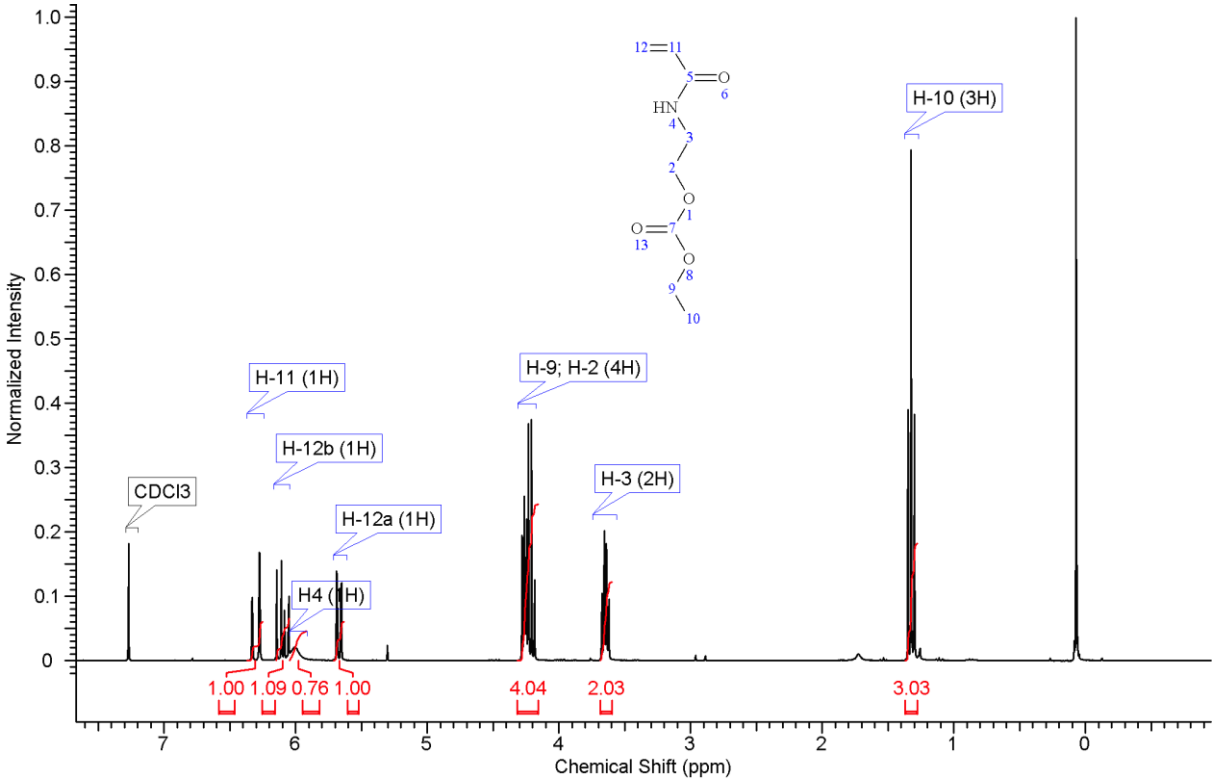

Figure S2. ^{1}H-NMR of HEAm-EC

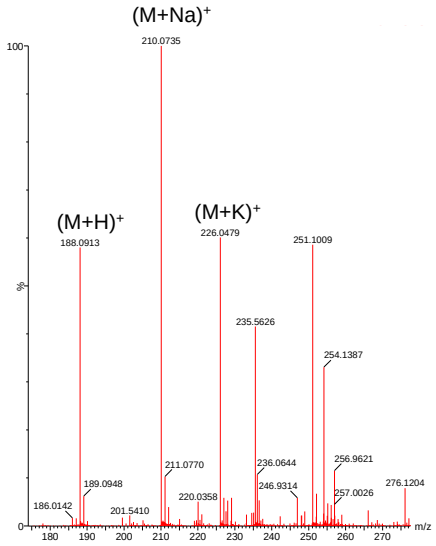

Figure S3. ESI-MS of HEAm-EC

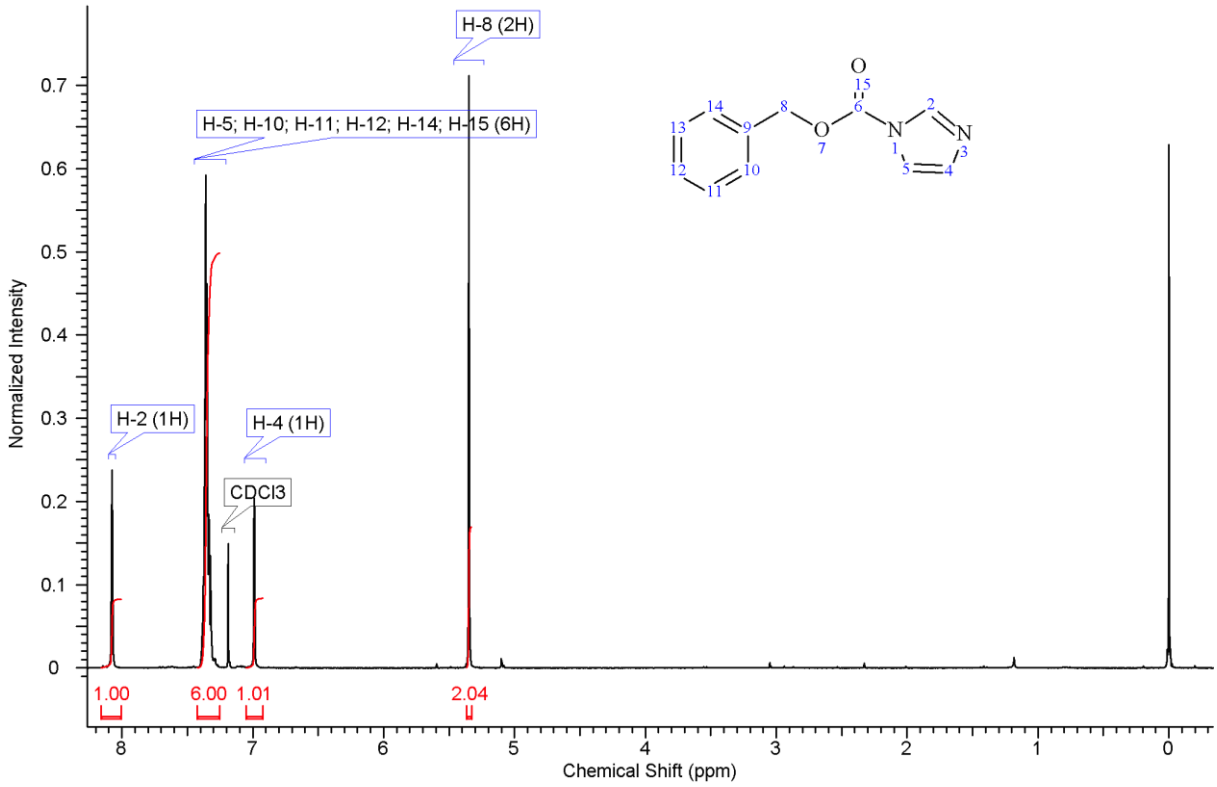

Figure S4. ^{1}H-NMR of Cl-activated benzylalcohol

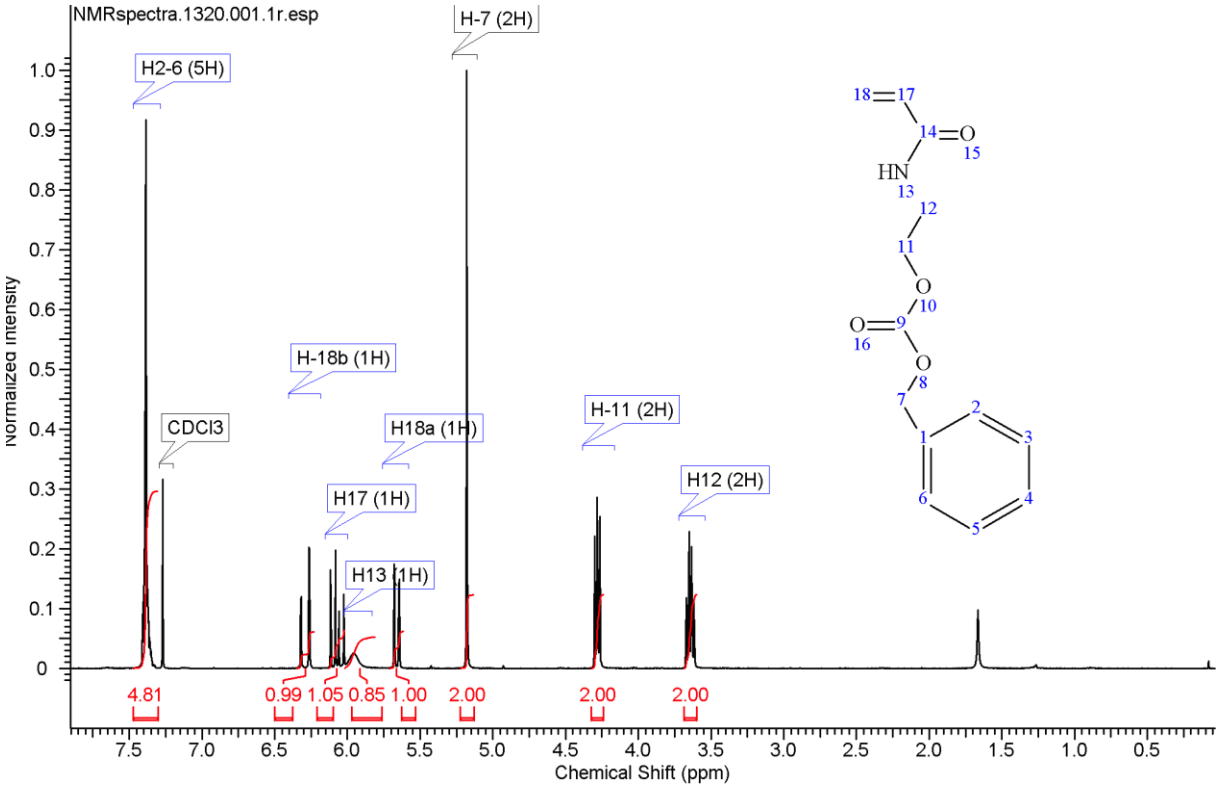

Figure S5. ^{1}H-NMR of HEAm-BC

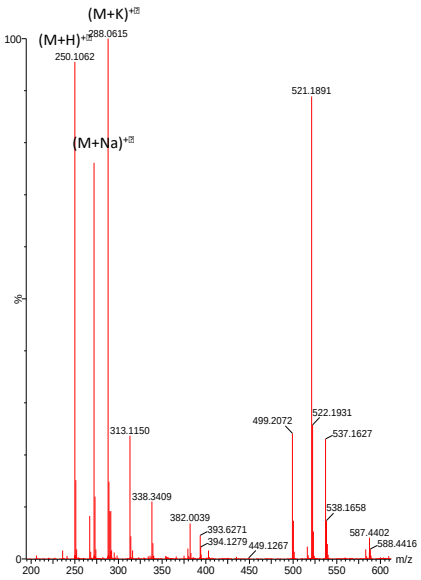

Figure S6. ESI-MS of HEAm-BC

Table S1. Supramolecular characteristics of synthesized block copolymers.

Polymer	Volume mean (nm)[a]	Đ[a]
$pHEAm_{64}$-$pHEAmEC_{26}$	10.99	0.36
$pHEAm_{64}$-$pHEAmEC_{56}$	32.12	0.16
$pHEAm_{140}$-$pHEAmEC_{88}$	44.63	0.036
$pHEAm_{140}$-$pHEAmEC_{160}$	86.47	0.13
PEG-$pHEAmEC_{41}$	29.33	0/12
PEG-$pHEAmEC_{81}$	46.33	0.10
$pHEAm_{64}$-$pHEAmBC_{25}$	27.40	0.26
$pHEAm_{64}$-$pHEAmBC_{68}$	65.22	0.32
$pHEAm_{140}$-$pHEAmBC_{91}$	94.69	0.40
$pHEAm_{140}$-$pHEAmBC_{192}$	91.54	0.27
PEG-$pHEAmBC_{42}$	35.56	0/081
PEG-$pHEAmBC_{78}$	101.23	0.050

[a] Numeric values of volume mean and Đ, measured by DLS at 25°C (n=3)

Table S2. Overview of CMC values and polymer concentrations in the samples used for the MTT assay.

PTX-concentration	pHEAM64-pHEAMEC26	pHEAM64-pHEAMBC25	pHEAM64-pHEAMEC56	pHEAM64-pHEAMBC68	PEG-pHEAMEC41	PEG-pHEAMBC42	PEG-pHEAMEC81	PEG-pHEA
(µM)	mg/mL	mg/mL	mg/mL	mg/mL	mg/mL	mg/mL	mg/mL	m
CMC (mg/mL)	**0.081 ± 0.03**	**0.024 ± 0.002**	**0.031 ± 0.002**	**0.0047 ± 0.0004**	**0.023 ± 0.004**	**0.0036 ± 0.0006**	**0.0096 ± 0.003**	**0.003 0.000**
2	1,71	0,688	0,516	0,152	0,208	0,0368	0,042	
1	0,855	0,344	0,258	0,076	0,104	0,0184	0,021	
0,1	0,085	0,034	0,0258	0,0076	0,0104	0,00184	0,0021	
0,01	0,0085	0,0034	0,00258	0,00076	0,00104	0,000184	0,00021	
0,001	0,00085	0,00034	0,000258	0,000076	0,000104	0,0000184	0,000021	0
0,0001	0,000085	0,000034	0,0000258	0,0000076	0,0000104	0,00000184	0,0000021	0,
0,00001	0,0000085	0,0000034	0,00000256	0,0000076	0,00000104	0,000000184	0,00000021	0,0